Neurons in cortical area MST remap the memory trace of visual motion across saccadic eye movements

Naoko Inaba[a,b,1] and Kenji Kawano[a]

[a]Department of Integrative Brain Science, Graduate School of Medicine, and [b]Research and Educational Unit of Leaders for Integrated Medical System, Center for the Promotion of Interdisciplinary Education and Research, Kyoto University, Kyoto 606-8501, Japan

Perception of a stable visual world despite eye motion requires integration of visual information across saccadic eye movements. To investigate how the visual system deals with localization of moving visual stimuli across saccades, we observed spatiotemporal changes of receptive fields (RFs) of motion-sensitive neurons across periods of saccades in the middle temporal (MT) and medial superior temporal (MST) areas. We found that the location of the RFs moved with shifts of eye position due to saccades, indicating that motion-sensitive neurons in both areas have retinotopic RFs across saccades. Different characteristic responses emerged when the moving visual stimulus was turned off before the saccades. For MT neurons, virtually no response was observed after the saccade, suggesting that the responses of these neurons simply reflect the reafferent visual information. In contrast, most MST neurons increased their firing rates when a saccade brought the location of the visual stimulus into their RFs, where the visual stimulus itself no longer existed. These findings suggest that the responses of such MST neurons after saccades were evoked by a memory of the stimulus that had preexisted in the postsaccadic RFs ("memory remapping"). A delayed-saccade paradigm further revealed that memory remapping in MST was linked to the saccade itself, rather than to a shift in attention. Thus, the visual motion information across saccades was integrated in spatiotopic coordinates and represented in the activity of MST neurons. This is likely to contribute to the perception of a stable visual world in the presence of eye movements.

The inhomogeneous visual resolution of the retina requires eye motion by saccadic eye movements to look around the environment. However, despite the frequent occurrences of saccades, humans are able to perceive the visual world as stable and continuous. Because each saccade changes the retinal locations of visual objects in the external world, the retinotopic representation of the visual scene in the brain must be overwritten by a new one according to each new eye position. One possible solution for the visual system to overcome such repetitions and to maintain perceptual continuity across saccades is to integrate the visual information before and after eye movement. As the neuronal correlate of the integration across saccades, so-called "remapping" of the visual scene has been reported in several visual areas, including the lateral intraparietal cortex (LIP), frontal eye field (FEF), and superior colliculus (SC). This emphasizes the predictive shift of the receptive field (RF) of the neuron to the location into which the developing saccade would bring the stimulus (1–6). However, the changes of the spatiotemporal characteristics of the RF have yet to be explored and are essential information for understanding the integration across the period of saccades.

To examine how the visual system deals with localization of moving visual stimuli across saccades, we carried out continuous observation of the RFs of neurons in the motion-sensitive cortical areas of monkeys: the middle temporal (MT) and medial superior temporal (MST) areas (7). Single-unit activities were recorded while the animals performed fixation and saccade tasks in which a spatially stable moving stimulus was presented in various visual fields. The moving stimulus was presented for long (600 ms) and short (170 ms) durations to allow observation of

spatiotemporal RF maps throughout the period of saccades and to examine possible RF-remapping across saccades, respectively.

Results

The activities of 187 neurons (141 in MST and 46 in MT) were studied in two monkeys. All of these neurons responded to a moving grating with directional selectivity. To locate the RF of each neuron, a moving grating was presented in a narrow vertical (or horizontal) strip at 1 of 20 locations divided horizontally or vertically (Fig. 1 A and B). The grating inside the strip was moved in each neuron's preferred direction (horizontal or vertical). To reduce the effects of retinal motion induced by the saccade itself, the RF was studied across the period of saccades that was parallel to the axis of the grating pattern.

MST Neurons Have Retinotopic Receptive Fields Even via Saccades. Sample responses of an MST neuron are shown in Fig. 1. The location of the neuron's RF defined by a moving random-dot pattern was close to the center of the screen but not covering the fovea, and had an area of about $17° \times 18°$ (Fig. 1C). In paradigm I, the grating pattern was displayed for 600 ms and in this case moved upward (Fig. S1A) at 20°/s (Fig. 1 D–F). Responses to the moving grating presented in a vertical strip at 20 locations (H1–H20, Fig. 1B) were observed. Fig. 1D shows the time course of the responses to the moving grating located at H1–H20, which reveals the spatiotemporal characteristic of the neuron's RF in the fixation task. The moving grating located at H7–H11 (inside RF) activated the neuron, but that outside the RF did not (at H1–H6, H12–H20). For example, when the strip with the moving grating was presented at H10 inside the RF, the neuron increased its activity ~40 ms after the stimulus onset (Fig. 1D, Right). The
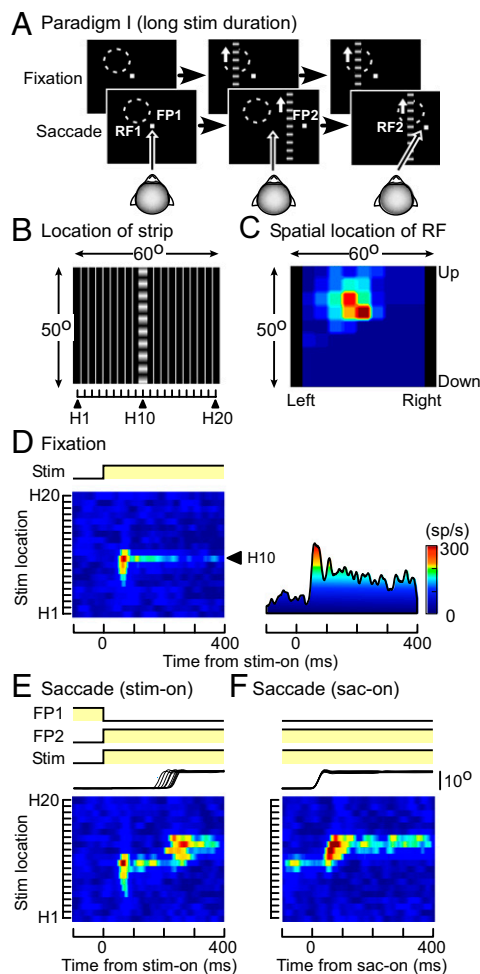
NEUROSCIENCE

Fig. 1. Responses of an MST neuron to a long duration stimulus (paradigm I). (*A*) Schematic diagram showing the sequence of paradigm I. (*Upper*) Fixation task: The monkey was required to keep its eyes fixed on a target at the screen center. A moving grating in a narrow vertical (or horizontal) strip was presented. (*Lower*) Saccade task: When the monkey maintained fixation for 400 ms, the fixation point (FP1) disappeared and a saccade target (FP2) and moving grating in a narrow vertical (or horizontal) strip appeared at the same time. The saccade target was located at 10° eccentricity on the horizontal (or vertical) axis. Receptive fields 1 and 2 (RF1 and RF2) are the locations of the RF of the neuron before and after the saccade, respectively. (*B*) Schematic diagram showing the screen where the moving grating was presented in a narrow vertical strip (3° width) at 1 of 20 locations divided horizontally (at H10). H1: left end; H20: right end. (*C*) Location of the RF of an MST neuron defined by a moving random-dot pattern. (*D*) (*Right*) Spike-density function in response to the moving grating at H10. (*Left*) Spatiotemporal RF map of the MST neuron during fixation. Responses at H1–H20 are aligned at the stimulus onset and lined up from bottom (H1) to top (H20). *x* axis: time from stimulus onset (in milliseconds); *y* axis: stimulus location from left to right (H1 to H20). The firing rate of the neuron is coded by color, as indicated in the right side bar. (*E* and *F*) Spatiotemporal RF map of the MST neuron during rightward 10° saccade. Each cartoon is a time line showing the status of the lights at FP1 (initial fixation target), FP2 (saccade target) and moving grating displayed at one of the 20 locations, and horizontal eye position. Upward indicates light-on or rightward. Responses are aligned at stimulus onset (*E*) or saccade onset (*F*). The moving grating was displayed throughout the periods before, during, and after the saccade.

RF location remained at the same place and the response magnitude and the RF size waned with the passage of time.

In the saccade task, when the fixation-target (FP1) was turned off, the saccade-target (FP2) and the moving grating were turned on at the same time (Fig. 1 *A* and *E*). Because the grating was

displayed for 600 ms, it was visible throughout the periods before, during, and after the saccade. If the RF of the neuron is represented in retinotopic coordinates, a saccade would shift the location of the RF on the screen from RF1 (presaccadic RF in Fig. 1*A*) to RF2 (postsaccadic RF in Fig. 1*A*), following the shift of the eye position. Such a shift was observed in the responses of the neuron in Fig. 1. When the animal fixated on FP1 and the strip with the moving grating was displayed at H7–H11 (inside RF1), the neuron increased its activity ~40 ms after the stimulus onset, and then the responses waned before the saccade (Fig. 1*E*). In contrast, when the strip with the moving grating was displayed at H10–H14 (inside RF2), the neuron increased its firing rate after the saccade. No responses were observed throughout the trials when the stimulus was placed outside RF1 and RF2, indicating that the saccade itself did not evoke any response in this neuron. The time course of the responses at H1–H20 shown in Fig. 1*E* indicates that the responses before the saccades were similar to those in the fixation task and that the shift of the RF location on the screen after the saccades was 10°, similar to the saccade size. As shown in Fig. 1*F*, the abrupt increase of the neuron's activity after the saccade is clearly seen when the responses were aligned at the onset of the saccades, which brought the strip with the moving grating at H10–H14 (inside RF2) into the RF. Furthermore, aligning the responses at the beginning of the saccades emphasizes the similarity between the spatiotemporal characteristic of the responses and the saccadic shift of the eye position. A similar shift of the RF location (leftward 10°) was also observed during 10° leftward saccades (Fig. S1 *B* and *C*). Thus, when the animal made a saccade, the RF location moved as if to follow the saccade, indicating that it was represented in retinotopic coordinates across the saccade. Similar results were observed in other MST neurons. After the saccade, almost all MST neurons (116 of 118) significantly responded to the stimulus in RF2 (two-sided Wilcoxon rank sum, $P < 0.05$; SI Text, Spatial Tuning Curves of the Neuronal Responses and Fig. S2), and the shift of its RF location on the screen was 9.6 ± 1.8°, similar to the saccade size (10°).

MST Neurons Remap Memory Trace Across Saccades. To test the assumption that neuronal responses after saccades simply reflect reafferent visual information, we carried out another fixation/saccade task (paradigm II; Fig. 2*A*), in which the moving grating was visible only before the saccades. In the fixation task, the responses of the neuron were similar to those to long-duration stimuli (in paradigm I; Fig. 1*D*), except for the shorter duration (Fig. 2*B*). In the saccade task, the location of the RF on the screen was expected to shift from RF1 to RF2 after the saccade (Fig. 2*A*). As in paradigm I, responses to the moving grating before the saccades were observed only when the strip was located inside RF1 (at H7–H11) (Fig. 2*C*). However, the neuron transiently increased its activity after the saccades when the strip had been displayed inside RF2 (at H12–H14) and turned off before the saccades (Fig. 2 *C* and *D*). That is, the neuron increased its activity when the location of the stimulus, which had preexisted on the screen, was moved into its RF by the saccade, even though the stimulus had already gone. When the responses were aligned at the beginning of the saccades, the neuron clearly responded to the preexisted stimulus after the saccade onset (Fig. 2*D*). In paradigm II, most MST neurons (66 of 98) significantly increased their firing rate in RF2 after the saccades (two-sided Wilcoxon rank sum, $P < 0.05$). It supports the assumption that the responses of MST neurons after saccades were evoked by a memory of the stimulus that had preexisted ("memory remapping"), although the amplitude of the neuronal response to the visual memory trace was weaker than that to the real stimulus (SI Text, Postresponse/Preresponse Ratio and Fig. S3).

Considering a possible effect of phosphor persistence of the cathode ray tube (CRT) display, we conducted additional experiments by using a mirror galvanometer system. We recorded 23 neurons in MST and obtained consistent results with the CRT
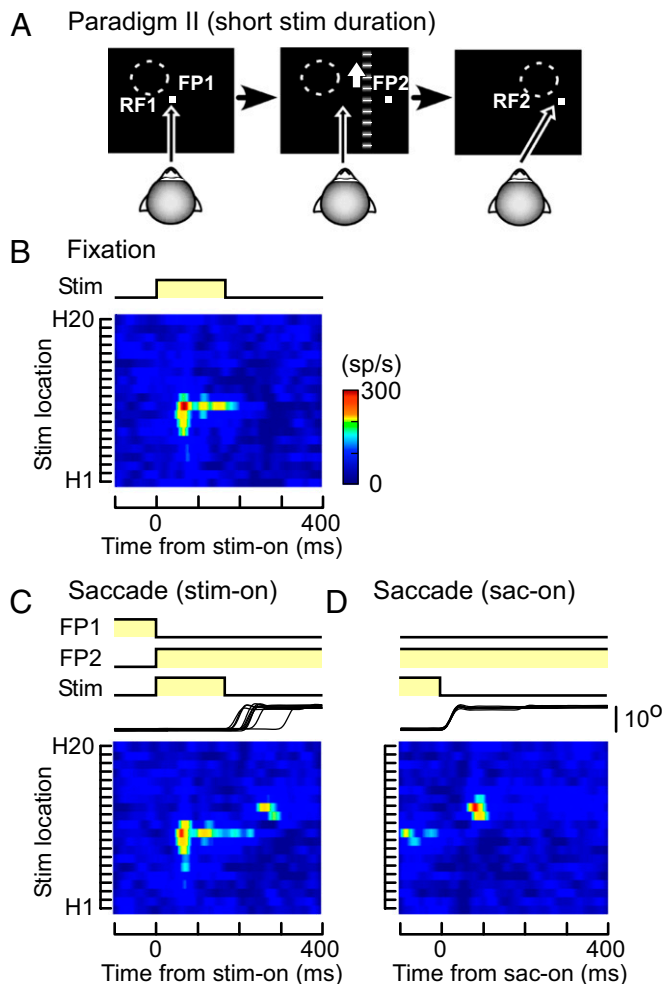
Fig. 2. Responses of the MST neuron to a short duration stimulus (paradigm II). (*A*) Schematic diagram showing the sequence of paradigm II. The moving grating was visible for 170 ms to make it vanish before the saccade onset. (*B–D*) Spatiotemporal RF maps of the MST neuron shown in Fig. 1 during fixation (*B*) and across the period of saccades (*C* and *D*). Responses are aligned at stimulus onset (*B* and *C*) or saccade onset (*D*). RF map, stimulus, and eye traces are as in Fig. 1.

experiments (*SI Text, Effect of Phosphor Persistence of the Cathode Ray Tube Display* and Fig. S4).

Memory Remapping in MST Is Dependent on Execution of Saccades. To examine whether memory remapping in MST is dependent on execution of the saccade itself or attention to the saccade target, we carried out a third saccade task (paradigm III). The monkey was required to perform delayed saccades, in which the saccade target (FP2) was turned on 300 ms before the stimulus onset and extinction of FP1 (Fig. 3*A*). As a result, the monkey had to wait until extinction of FP1 to execute the saccade while paying attention to FP2 (8). The moving grating was turned off before the saccade onset, as in paradigm II.

When the monkey fixated on FP1 and the strip with the moving grating was displayed in RF1, the neuron increased its firing rate (Fig. 3*B*). However, when the strip was displayed in RF2, no responses were observed before the saccades even though the monkey could anticipate the consequence of the intended saccades before appearance of the stimulus (Fig. 3*B*). It supports the idea that memory remapping in MST is dependent on execution of the saccade itself. By aligning the responses at the saccade onset, the neuron's increased activity after the saccade was more pronounced (Fig. 3*C*). In paradigm III, most

MST neurons (31 of 42) significantly increased their activity in RF2 after the saccades (two-sided Wilcoxon rank sum, $P < 0.05$).

Thus, the RFs of MST neurons in memory trace were remapped along the trajectory of a saccade, so that the stimulus in the future RFs as defined by the saccade activated the neuron after the time of the saccade. Previous studies in other areas, such as LIP and FEF, found neurons increasing their activities in relation to visual stimuli presented in their future RFs before saccades, a process referred to as "predictive remapping" (1). However, we encountered very few neurons (2 of 135) that showed such predictive remapping before saccades in MST. Almost all MST neurons began to discharge in response to the moving grating in their postsaccadic RF (RF2) only after the saccade onset, and their responses to the moving grating before the saccades were observed only when the moving grating was located inside their presaccadic RF (RF1).

Spatiotemporal Receptive Field Map of MT Neurons. The results above indicate that MST neurons have retinotopic RFs across saccades and that the location of the RF on the screen moves with changes of eye position due to saccades. Furthermore, most MST neurons remap the memory trace across saccades, which is dependent on execution of the saccades. The MST receives most of its inputs from the MT, which is involved primarily in visual motion processing, and some MT neurons send outputs to FEF and LIP, which have activity related to the generation of saccades and remapping of their RFs. Therefore, we carried out the same tasks during recording of neuronal activities in MT. In Fig. 4, sample RF maps of an MT neuron are shown. The location of the RF defined by a moving random-dot pattern was close to the center of the screen but not covering the fovea, and its size was $<2° × 2°$ (Fig. 4*A*). Because the RF straddled the border between H10 and H11, the moving grating displayed in both strips activated the neuron and the RF location remained at the same place during fixation (Fig. 4 *B* and *E*). Similarly to the MST neuron in Fig. 1, in paradigm I, saccades shifted the location of the RF on the screen following the shift of the eye position (Fig. 4 *C* and *D*). It indicates that the MT neuron also has retinotopic RFs across saccades. In paradigm II, the responses to the moving grating presented in RF1 were similar in both the fixation and saccade tasks. (Fig. 4 *E* and *F*). In the saccade task, no response
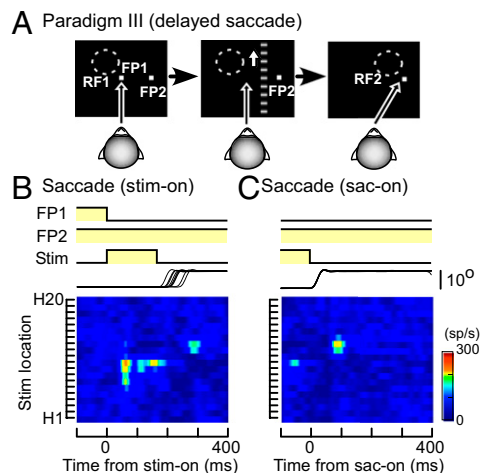
Fig. 3. Responses of the MST neuron during delayed saccades (paradigm III). (*A*) Schematic diagram showing the sequence of paradigm III. The saccade target (FP2) was turned on 300 ms before onset of the moving grating and offset of the fixation point (FP1). The moving grating was turned off before the saccade onset, as in paradigm II. (*B* and *C*) Spatiotemporal RF maps of the MST neuron shown in Figs. 1 and 2 across the period of saccades (*B* and *C*). Responses are aligned at stimulus onset (*B*) or saccade onset (*C*). RF map, stimulus, and eye traces are as in Fig. 1.

NEUROSCIENCE

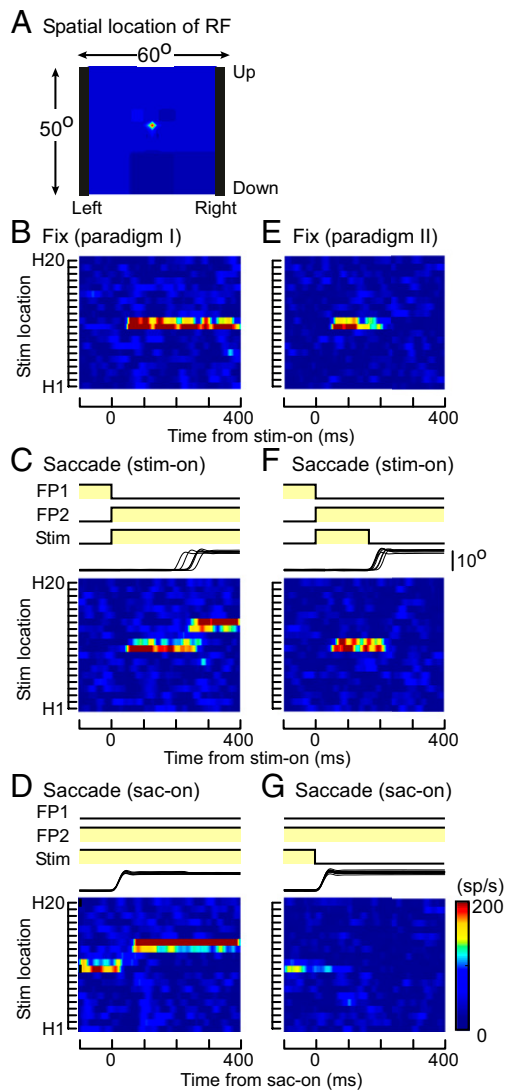**Fig. 4.** Responses of an MT neuron (paradigms I and II). (*A*) Location of the RF of an MT neuron defined by a moving random-dot pattern. (*B–D*) Spatiotemporal RF maps of the MT neuron during fixation (*B*) and across the period of saccades (*C* and *D*) in paradigm I. The moving grating was visible throughout the periods before, during, and after the saccade. (*E–G*) Spatiotemporal RF maps of the same MT neuron during fixation (*E*) and across the period of saccades (*F* and *G*) in paradigm II. The moving grating was turned off before the saccade onset. Responses are aligned at stimulus onset (*B*, *C*, *E*, and *F*) or saccade onset (*D* and *G*). RF map, stimulus, and eye traces are as in Fig. 1.

was observed after the saccade, even when the saccade brought the location of the stimulus, which had preexisted, into the RF2 (Fig. 4 *F* and *G*). Unlike most MST neurons, we did not find significant evidence of memory remapping for MT neurons. Actually no MT neurons responded to the preexisted turned-off stimulus in RF2 after the saccade in paradigm II (two-sided Wilcoxon rank sum, $P > 0.05$), although all of them (41 of 41) responded to the existing stimulus in RF2 after the saccade in paradigm I (two-sided Wilcoxon rank sum, $P < 0.05$).

Comparison Between MST and MT Neurons. Between MT and MST neurons, different response characteristics were observed when the moving visual stimulus was turned off before saccades (paradigm II). To quantify the neuronal characteristics for each neuron, we examined the "stimulus location" to which a neuron is sensitive during paradigm II. We applied a sliding-window

receiver operating characteristic (ROC) analysis to the spatial tuning of responses obtained from individual trials throughout the period of saccades (*Materials and Methods*). Fig. 5*A* illustrates the time course of the area under the ROC curves (AUC) as a classifier for the stimulus in presaccadic RF (RF1) and postsaccadic RF (RF2). For both MT ($n = 41$) and MST neurons ($n = 98$), the AUC for RF1 increased after the stimulus onset and remained high before the saccade and then waned after the saccade. For MST neurons, but not MT neurons, the AUC for RF2 significantly increased after the saccade offset, supporting the idea that MST, but not MT, neurons remap the memory trace of the visual stimulus across the saccade. The median AUC from 50 to 100 ms after the saccade offset for the 98 MST and 41 MT neurons was 0.77 ± 0.19 and 0.47 ± 0.17, respectively (two-sided Wilcoxon rank sum, $P < 0.01$; Fig. 5*B*).

The distributions of response latencies shown in Fig. 5*C* brought out a further contrast between the responses of MT and MST neurons. The response latencies were measured from stimulus onset at RF1 and from saccade offset at RF2. In paradigm I, the median values of the former was 45.0 ± 12.2 (ms) and the latter was 40.5 ± 13.6 (ms) for the MST neurons, which were significantly different from each other (two-sided Wilcoxon signed rank, $P < 0.01$, $n = 118$). Actually, most MST neurons (82 of 118) had latencies from the saccade offset that were shorter than those from the visual stimulus onset. In contrast, for MT neurons, the median values of latencies measured from stimulus onset and those from saccade offset were 39.4 ± 11.3 (ms) and 50.4 ± 22.5 (ms), respectively, and the former was significantly shorter than the latter (two-sided Wilcoxon signed-rank, $P < 0.01$, $n = 46$). Although the latencies for the MT neurons measured from stimulus onset were significantly shorter than those for the MST neurons (two-sided Wilcoxon rank sum, $P < 0.01$), the latencies for the MST neurons measured from saccade offset were significantly shorter than those for the MT neurons (two-sided Wilcoxon rank sum, $P < 0.01$).
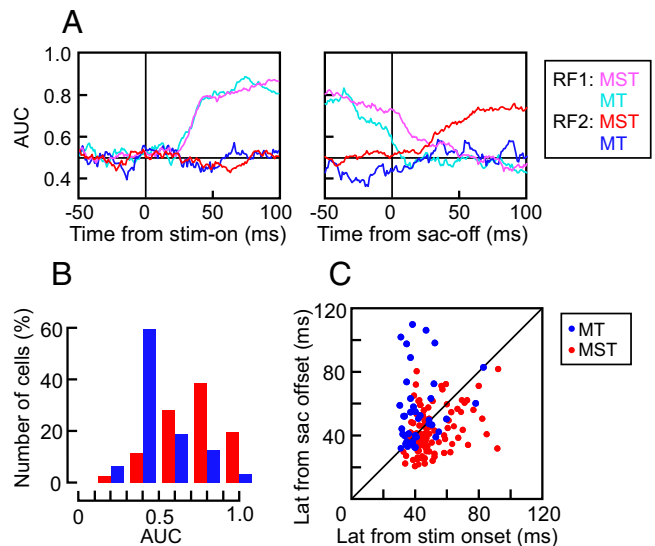

Fig. 5. Comparison between MST and MT neurons. (*A*) The time course of the AUC as a classifier for the stimulus in RF1 (MST: magenta; MT: cyan) and RF2 (MST: red; MT: blue). For MST neurons, but not MT neurons, the AUC for RF2 significantly increased after the saccade. (*B*) Distribution of the mean AUC from 50 to 100 ms after the saccade offset for the 98 MST (red bars) and 41 MT neurons (blue bars). (*C*) Relationship between the response latencies measured from stimulus onset at RF1 (abscissa) and from saccade offset at RF2 (ordinate) in paradigm I. Note that the latencies of MT neurons (blue dots) from stimulus onset were shorter than MST neurons (red dots), but the latencies of MT neurons from saccade offset were longer than MST neurons.

Discussion

We observed spatiotemporal changes of RFs of motion-sensitive neurons across the period of saccades in areas MT and MST and found that the motion-sensitive neurons in both areas have retinotopic RFs across the saccades. However, different characteristics in responses emerged when the moving visual stimulus was turned off before the saccades. For MT neurons, virtually no response was observed after the saccade, suggesting that the responses of these neurons simply reflect reafferent visual information, consistent with the previous findings (9, 10). In contrast, MST neurons increased their firing rates when a saccade brought the location of the visual stimulus into their RFs, where the visual stimulus itself no longer existed. This suggests that the responses of such MST neurons after saccades were evoked by memory of the stimulus that had preexisted in their postsaccadic RFs (memory remapping). A delayed-saccade paradigm (paradigm III) further showed that memory remapping in MST was linked to the saccade itself, rather than to an attention shift. Because the responses after saccades were evoked by memory of the visual stimulus that had gone in paradigms II and III, the RF remapping of the MST neurons was considered to be retrospective rather than predictive.

Two questions arise: how (or where) the stimulus that had preexisted in postsaccadic RFs is stored, and how (or from where) the saccade information that triggers recall of the stored visual information to be remapped is acquired. For the first question, one possibility is that MST neurons receive visual information from neurons with RFs that are fixed in spatiotopic, rather than retinal, coordinates. Electrophysiological studies have shown that neurons in area V6 (11), the ventral intraparietal area (VIP) (12) have RFs represented as spatial locations explicitly in a head-centered frame of reference. Both V6 and VIP have anatomical connections to MST and receive their visual input mainly from MT (7, 13, 14). The neural correlates of the visual information being maintained after its disappearance have yet to be studied in these regions, but we suggest that a saccade activates input providing maintained visual information in MST neurons with RF locations coinciding with the postsaccadic RF in spatiotopic coordinates. Another possibility is that MST neurons receive visual information in the postsaccadic RF (or future RF) before the time of a saccade. This so-called presaccadic or predictive remapping of RFs has been described in LIP (1, 15, 16), FEF (2, 6), SC (17–19), and some areas of the prestriate cortex (3, 20). In these areas, neurons that had postsaccadic visual memory responses but not predictive remapping were also recorded (3, 21–23). Because there are a considerable number of neurons showing predictive remapping in these areas, neurons with postsaccadic visual memory responses would receive maintained information of the visual stimulus from neighboring neurons. However, in the present study, we found very few neurons in MST that increased their activities in the future RFs before saccades. Thus, it is unlikely that visual responses elicited by predictive remapping before saccades were maintained in MST and recalled by saccades in spatiotopic coordinates. It is reasonable to assume that visual information in the future RF is provided by neurons in areas where both predictive and memory remapping have been frequently observed, such as LIP and FEF.

Regarding the second question, extraretinal signals coding eye movements in MST have been described. These signals are found during smooth pursuit (24–27) or to modulate neuronal responses in relation to eye positions (28–31), but it is possible that the extraretinal signals also provide information on saccades in MST. Thus, the results of the present study suggest that visual information before the saccade is retained and localized in spatiotopic coordinates in the upstream visual area(s) and that extraretinal signals coding the saccade-vector trigger its representation as neuronal activity in MST. The recalled information that had preexisted and the renewed information after saccades would be integrated, thus allowing perception of the visual world as stable and continuous. This proposal is consistent with psychological experiments on human subjects showing spatiotopic integration of

visual motion across saccades (32), although there is a critical explanation on their study, claiming that they result from a non-spatial reduction in uncertainty (33). Because our study did not require monkeys to make a decision, an experiment using similar visual stimuli (coherent/noncoherent random dots) might be necessary to directly compare our study to these psychophysical studies.

In previous studies (34), the neurons showing predictive remapping were mainly found in areas with a role in guiding quick, goal-directed motor actions such as saccades. The finding that only few neurons in MST showed predictive remapping before saccades is understandable in the view that this area has a different role, which is to perceive the visual world. The result that MST neurons responded to a stimulus located at the postsaccadic RF earlier than MT neurons (Fig. 5*C*) suggests that the recalled information might be used to fill the missing vision due to saccadic suppression in MT (35) and contribute to continuous and stable visual perception.

Materials and Methods

Animal Preparation. Two male rhesus monkeys (monkeys M and Y; *Macaca mulatta*) weighing 7 and 9 kg were used in this study. The Animal Care and Use Committee at Kyoto University approved all protocols as complying with the guidelines established in the Public Health Service *Guide for the Care and Use of Laboratory Animals* (36). The procedures used in the study were similar to those described elsewhere (24, 37). Standard methods were used to implant subconjunctival scleral search coils (38), head-restraining devices, and recording chambers during aseptic surgery performed under general anesthesia with ketamine and pentobarbital sodium. The recording chambers were stereotaxically placed to allow for a dorsal approach to the parietal cortex in the vertical orientation (stereotaxic coordinates: anterioposterior, −2 to −4 mm; mediolateral, ±16–18 mm), guided by T1 magnetic resonance imaging.

Recording Technique and Visual Stimuli. The animal sat in a primate chair in a dark room with the head fixed by a head holder and facing a 19-inch CRT monitor (FlexScan T766; Nanao), which was located 30 cm in front of the eyes. Visual stimuli were presented on the monitor [1,280 × 1,024 pixels (60° × 50°); refresh rate, 100 Hz]. The period of exposure to the visual stimulus was monitored by a photodiode (Sharp; SBC111) attached to the CRT monitor. Further details of this procedure have been described previously (39, 40).

Initial mapping of the cortex in the dorsal part of the superior temporal sulcus (STS) were made with hand-made glass-coated tungsten electrodes. MRI scans were used to confirm the location of the STS. Within the STS, MST or MT neurons were identified based on their location relative to the STS and their RF characteristics (41, 42) (see figure 1 in ref. 37 and supplemental figure 1 in ref. 25). Single units were recorded with tungsten microelectrodes (Microprobe or FHC) via transdural guide tubes inserted in the grid hole using a guide-tube grid system (Crist Instruments).

Having isolated a visual motion-sensitive neuron, we determined the neuron's preferred direction by observing its responses to a moving random-dot pattern (with selection of a suitable field size for each neuron: 50° × 50° to 2° × 2°) in eight directions (horizontal, vertical, and diagonal). We recorded the neuronal activity while the monkeys performed saccade/fixation tasks to map the location of their RFs. The visual stimulus was a sinusoidal grating pattern with spatial frequency of 0.6 cyc/° and moved at 20°/s vertically or horizontally, respectively. The orientation of the grating pattern was orthogonal to the neuron's preferred direction and always in parallel to the saccade axis. Because the CRT screen (60° × 50°) was divided into 20 strips (either horizontal or vertical) to map the location of the RF, the grating pattern occupied 1 of the 40 strips, which was horizontal (60° wide and 2.5° tall) or vertical (3° wide and 50° tall) (Fig. 1*A*). When the center of the RF was outside the CRT monitor or the border of the RF could not be defined, further recordings were aborted. The neurons, which responded to the saccade to the target (FP2), were also excluded from further analysis.

Behavioral Paradigms. Three paradigms consisting of fixation/saccade tasks were designed. Paradigm I consisted of a simple fixation/visually guided saccade task (Fig. 1*A*). Each trial started when a fixation point (FP1) appeared at the center of the screen. In the saccade trial, if the monkey maintained fixation in a 1.5° × 1.5° window for 400 ms, a saccade target (FP2) and a moving grating appeared at the same time as the fixation point disappeared. The saccade target was located at 10° eccentricity on the horizontal or vertical axis. The monkey had to make a saccade immediately after FP1 disappeared. Further recordings were aborted if monkey did not start the saccade by the time 300 ms after offset of FP1. To define the RF, a strip containing the moving grating was positioned at 1 of the 40 locations

divided horizontally and vertically (Fig. 1*B*). In the saccade task of paradigm I, the moving grating remained visible for 600 ms, including the entire time during the saccade. In contrast, in the saccade task of paradigm II, the moving grating was visible for 170 ms to make it vanish before the saccade onset (Fig. 2*A*). In the saccade task of paradigm III, the monkeys were required to have a delayed saccade (Fig. 3*A*). FP2 came 300 ms before onset of the moving grating and offset of FP1. If the monkey broke fixation before FP1 was turned off, the trial ended without reward. To receive a fruit juice reward, the monkey was required to keep its eyes within 1.5° of FP1 (fixation task) or FP2 (saccade task) until the target disappeared. In paradigms II and III, because we rejected trials in which the saccadic latency was shorter than 170 ms, the analyzed data were taken when the animal did not see the visual stimuli during and after the saccades.

Data Collection and Analysis. All data analysis programs were written in MATLAB (MathWorks). Stimulus presentation and data collection were controlled by a personal computer using the REX system (43). A time-amplitude window discriminator was used to identify spikes with a time resolution of 1 ms. Spike-density functions were calculated by convolving the spike trains with a Gaussian curve ($\sigma = 10$ ms) (44). To evaluate the neuronal response, the firing rate of each neuron was averaged over a time period of 50–150 ms after stimulus onset or 50–150 ms after the saccade onset. The response latency was taken when the spike density function exceeded the mean plus 2SD of spontaneous activity and stayed above this threshold for the subsequent 25 ms. The details of the analysis were similar to those described previously (45).

To determine the response characteristics for each neuron, we examined the "location" of the visual stimulus that activated the neuron during paradigm II. As a result, we found that the RF moved from the presaccadic RF (RF1) to the postsaccadic RF (RF2) with changes of eye position due to saccades. The RF1 and RF2 were defined as spatial tuning of the neuronal responses measured from the average spike density from 50 to 170 ms after the stimulus onset, and that from 50 to 200 ms after the saccade offset in paradigm I, respectively. A sliding-window ROC analysis was applied to the spatial tuning of neural responses obtained from individual trials throughout the period of saccades in paradigm II (46). The spatial tuning of neuronal responses to the stimulus located at 20 locations was measured within a 10-ms time window sliding at 1-ms steps for each neuron. Two ROC curves were obtained with each step: one as a classifier for stimulus in RF1 and the other as a classifier for stimulus in RF2. Then, the AUC was calculated for each ROC curve to compute the time course of the neuron's performance (25, 47).

1. Duhamel JR, Colby CL, Goldberg ME (1992) The updating of the representation of visual space in parietal cortex by intended eye movements. *Science* 255(5040):90–92.
2. Umeno MM, Goldberg ME (1997) Spatial processing in the monkey frontal eye field. I. Predictive visual responses. *J Neurophysiol* 78(3):1373–1383.
3. Nakamura K, Colby CL (2002) Updating of the visual representation in monkey striate and extrastriate cortex during saccades. *Proc Natl Acad Sci USA* 99(6):4026–4031.
4. Krekelberg B, Kubischik M, Hoffmann KP, Bremmer F (2003) Neural correlates of visual localization and perisaccadic mislocalization. *Neuron* 37(3):537–545.
5. Kusunoki M, Goldberg ME (2003) The time course of perisaccadic receptive field shifts in the lateral intraparietal area of the monkey. *J Neurophysiol* 89(3):1519–1527.
6. Sommer MA, Wurtz RH (2006) Influence of the thalamus on spatial visual processing in frontal cortex. *Nature* 444(7117):374–377.
7. Maunsell JH, van Essen DC (1983) The connections of the middle temporal visual area (MT) and their relationship to a cortical hierarchy in the macaque monkey. *J Neurosci* 3(12):2563–2586.
8. Colby CL, Goldberg ME (1999) Space and attention in parietal cortex. *Annu Rev Neurosci* 22:319–349.
9. Ong WS, Bisley JW (2011) A lack of anticipatory remapping of retinotopic receptive fields in the middle temporal area. *J Neurosci* 31(29):10432–10436.
10. Hartmann TS, Bremmer F, Albright TD, Krekelberg B (2011) Receptive field positions in area MT during slow eye movements. *J Neurosci* 31(29):10437–10444.
11. Galletti C, Battaglini PP, Fattori P (1993) Parietal neurons encoding spatial locations in craniotopic coordinates. *Exp Brain Res* 96(2):221–229.
12. Duhamel JR, Bremmer F, Ben Hamed S, Graf W (1997) Spatial invariance of visual receptive fields in parietal cortex neurons. *Nature* 389(6653):845–848.
13. Lewis JW, Van Essen DC (2000) Corticocortical connections of visual, sensorimotor, and multimodal processing areas in the parietal lobe of the macaque monkey. *J Comp Neurol* 428(1):112–137.
14. Baizer JS, Ungerleider LG, Desimone R (1991) Organization of visual inputs to the inferior temporal and posterior parietal cortex in macaques. *J Neurosci* 11(1):168–190.
15. Heiser LM, Colby CL (2006) Spatial updating in area LIP is independent of saccade direction. *J Neurophysiol* 95(5):2751–2767.
16. Heiser LM, Berman RA, Saunders RC, Colby CL (2005) Dynamic circuitry for updating spatial representations. II. Physiological evidence for interhemispheric transfer in area LIP of the split-brain macaque. *J Neurophysiol* 94(5):3249–3258.
17. Walker MF, Fitzgibbon EJ, Goldberg ME (1995) Neurons in the monkey superior colliculus predict the visual result of impending saccadic eye movements. *J Neurophysiol* 73(5):1988–2003.
18. Dunn CA, Hall NJ, Colby CL (2010) Spatial updating in monkey superior colliculus in the absence of the forebrain commissures: Dissociation between superficial and intermediate layers. *J Neurophysiol* 104(3):1267–1285.
19. Churan J, Guitton D, Pack CC (2011) Context dependence of receptive field remapping in superior colliculus. *J Neurophysiol* 106(4):1862–1874.
20. Tolias AS, et al. (2001) Eye movements modulate visual receptive fields of V4 neurons. *Neuron* 29(3):757–767.
21. Colby CL, Duhamel JR, Goldberg ME (1995) Oculocentric spatial representation in parietal cortex. *Cereb Cortex* 5(5):470–481.
22. Nakamura K, Colby CL (2000) Visual, saccade-related, and cognitive activation of single neurons in monkey extrastriate area V3A. *J Neurophysiol* 84(2):677–692.
23. Umeno MM, Goldberg ME (2001) Spatial processing in the monkey frontal eye field. II. Memory responses. *J Neurophysiol* 86(5):2344–2352.
24. Inaba N, Shinomoto S, Yamane S, Takemura A, Kawano K (2007) MST neurons code for visual motion in space independent of pursuit eye movements. *J Neurophysiol* 97(5):3473–3483.
25. Inaba N, Miura K, Kawano K (2011) Direction and speed tuning to visual motion in cortical areas MT and MSTd during smooth pursuit eye movements. *J Neurophysiol* 105(4):1531–1545.
26. Sakata H, Shibutani H, Kawano K (1983) Functional properties of visual tracking neurons in posterior parietal association cortex of the monkey. *J Neurophysiol* 49(6):1364–1380.
27. Newsome WT, Wurtz RH, Komatsu H (1988) Relation of cortical areas MT and MST to pursuit eye movements. II. Differentiation of retinal from extraretinal inputs. *J Neurophysiol* 60(2):604–620.
28. Morris AP, Kubischik M, Hoffmann KP, Krekelberg B, Bremmer F (2012) Dynamics of eye-position signals in the dorsal visual system. *Curr Biol* 22(3):173–179.
29. Morris AP, Bremmer F, Krekelberg B (2013) Eye-position signals in the dorsal visual system are accurate and precise on short timescales. *J Neurosci* 33(30):12395–12406.
30. Andersen RA, Essick GK, Siegel RM (1985) Encoding of spatial location by posterior parietal neurons. *Science* 230(4724):456–458.
31. Andersen RA, Mountcastle VB (1983) The influence of the angle of gaze upon the excitability of the light-sensitive neurons of the posterior parietal cortex. *J Neurosci* 3(3):532–548.
32. Melcher D, Morrone MC (2003) Spatiotopic temporal integration of visual motion across saccadic eye movements. *Nat Neurosci* 6(8):877–881.
33. Morris AP, et al. (2010) Summation of visual motion across eye movements reflects a nonspatial decision mechanism. *J Neurosci* 30(29):9821–9830.
34. Wurtz RH (2008) Neuronal mechanisms of visual stability. *Vision Res* 48(20):2070–2089.
35. Berman RA, Wurtz RH (2011) Signals conveyed in the pulvinar pathway from superior colliculus to cortical area MT. *J Neurosci* 31(2):373–384.
36. Committee for the Update on the *Guide for the Care and Use of Laboratory Animals* (2011) *Guide for the Care and Use of Laboratory Animals* (The National Academies Press, Washington, DC), 8th Ed.
37. Kawano K, Shidara M, Watanabe Y, Yamane S (1994) Neural activity in cortical area MST of alert monkey during ocular following responses. *J Neurophysiol* 71(6):2305–2324.
38. Judge SJ, Richmond BJ, Chu FC (1980) Implantation of magnetic search coils for measurement of eye position: An improved method. *Vision Res* 20(6):535–538.
39. Sheliga BM, Chen KJ, Fitzgibbon EJ, Miles FA (2005) Initial ocular following in humans: A response to first-order motion energy. *Vision Res* 45(25-26):3307–3321.
40. Miura K, et al. (2006) The visual motion detectors underlying ocular following responses in monkeys. *Vision Res* 46(6-7):869–878.
41. Gattass R, Gross CG (1981) Visual topography of striate projection zone (MT) in posterior superior temporal sulcus of the macaque. *J Neurophysiol* 46(3):621–638.
42. Komatsu H, Wurtz RH (1988) Relation of cortical areas MT and MST to pursuit eye movements. I. Localization and visual properties of neurons. *J Neurophysiol* 60(2):580–603.
43. Hays AV, Richmond BJ, Optican LM (1982) A UNIX-based multiple process system for real-time data acquisition and control. *WESCON Conference Proceedings* 2(1):1–10.
44. Richmond BJ, Optican LM, Podell M, Spitzer H (1987) Temporal encoding of two-dimensional patterns by single units in primate inferior temporal cortex. I. Response characteristics. *J Neurophysiol* 57(1):132–146.
45. Inaba N, Kawano K (2010) Responses of MSTd and MT neurons during smooth pursuit exhibit similar temporal frequency dependence on retinal image motion. *Cereb Cortex* 20(7):1708–1718.
46. Britten KH, Shadlen MN, Newsome WT, Movshon JA (1992) The analysis of visual motion: A comparison of neuronal and psychophysical performance. *J Neurosci* 12(12):4745–4765.
47. Fawcett T (2006) An introduction to ROC analysis. *Pattern Recognit Lett* 27(8):861–874.

Supporting Information

Inaba and Kawano 10.1073/pnas.1401370111

SI Text

Spatial Tuning Curves of the Neuronal Responses. To characterize the neuron's spatial tuning profile for each of the behavioral conditions, we quantified the neuronal responses to the moving stimulus located at 20 locations. We fitted a Gaussian function involving four free parameters to the neuronal responses obtained from individual trials over a time period of 50–150 ms after stimulus onset and 50–150 ms after saccade onset (Fig. S2) as follows:

$$y(\theta) = B + A \cdot \exp\left\{-0.5 \cdot ((\theta - \theta_0)/\sigma)^2\right\}, \qquad [\text{S1}]$$

where B, A, θ_0, and σ denote the baseline firing rate, maximal amplitude, optimal location, and tuning width, respectively (1). The parameter values of the best-fit function were used to quantify the spatial tuning profiles. We defined the stimulus location inside and outside the receptive field (RF) as within the range between $\theta_0 \pm \sigma^2$ and out of the range between $\theta_0 \pm 3\sigma^2$, respectively. We regarded a neuron as having significantly increased its firing rate if the mean response in the RF was larger than the mean plus 2SD of baseline activity out of the RF. As a robust test of statistical significance, we have used two-sided Wilcoxon rank sum tests between the mean responses inside and outside the RF.

Postresponse/Preresponse Ratio. To assess the influence of saccades on neuronal responses, we calculated a postresponse/preresponse ratio (defined as $[(R_{post}/R_{pre})] \times 100\%$), where R_{post} and R_{pre} are the mean firing rates after the saccade (50–150 ms after saccade onset) and before the saccade (50–150 ms after stimulus onset), respectively (Fig. S3). A small positive value (<100%) indicates that the response after the saccade is weaker than that after the stimulus onset. In paradigm I, when the moving grating was turned on in the RF (RF1) or brought into the RF by saccades (RF2), relatively similar responses were observed for neurons recorded in medial superior temporal (MST) area ($n = 118$, ratio = $89.7 \pm 34.5\%$; median $\pm$ SD) and middle temporal (MT) area ($n = 46$, ratio = $90.7 \pm 56.1\%$; median $\pm$ SD) (Fig. S3A, two-sided Wilcoxon rank-sum, $P > 0.05$). There were some neurons in both areas that had a small value of the postresponse/preresponse ratio (50% or less), as they showed very strong responses to the onset of the moving grating but not as large responses when the saccade brought the stimulus into their RF. However, on average in paradigm I, the neuronal population responded to the stimulus similarly (~90%) when the visual stimulus was turned on in the RF and when the saccade brought the stimulus into the RF.

In contrast, in paradigm II, when the moving grating was turned off before saccades, virtually no response was observed after saccade in MT neurons ($n = 41$, ratio = $10.2 \pm 7.5\%$; median $\pm$ SD; Fig. S3B). However, most MST neurons discharged when a saccade brought the location of the visual stimulus into their RFs, where the visual stimulus itself was no longer presented at that time. The mean amplitude of the neuronal response to the visual memory trace was weaker than that to the real stimulus ($n = 98$, ratio = $53.4 \pm 34.5\%$; median $\pm$ SD; Fig. S3B), significantly different from MT (two-sided Wilcoxon rank sum, $P < 0.01$). Similar effects of the saccades on the responses of MST ($n = 42$, ratio = $53.9 \pm 26.1\%$; median $\pm$ SD) and MT ($n = 12$, ratio = $18.1 \pm 5.6\%$; median $\pm$ SD) neurons were observed in paradigm III (Fig. S3C; two-sided Wilcoxon rank sum, $P < 0.01$).

Effect of Phosphor Persistence of the Cathode Ray Tube Display. In consideration of the effect of phosphor persistence of the cathode ray tube (CRT) display that might cause neuronal responses to the visual stimulus that had been turned off a while ago, we conducted additional experiments by using a mirror galvanometer system with a mechanical shutter (paradigms I-2 and II-2). The procedures used in the present study are similar to those previously described (2).

The animal was seated in a dark room and faced a translucent tangent screen subtending 80° × 80° at the viewing distance of 40 cm. A red spot (the fixation point or saccade target, 0.3° in diameter) and a grating pattern were backprojected onto the screen by a light-emitting diode projector and a slide projector, respectively. The sinusoidal grating pattern with spatial frequencies of 0.6 cyc/° were moved with mirror galvanometers in the light paths (Fig. 1A). To map the location of the RF, the moving grating pattern was presented in a narrow strip, which was horizontal (80° wide and 4° tall) or vertical (4° wide and 80° tall) as dividing the size of screen into 20 strips (either horizontal or vertical). An electromechanical shutter in the light path was used to turn the grating stimulus on and off (opening and closing time, <5 ms). The task sequence was the same between paradigm I and paradigm I-2 (Fig. 1A). Between paradigm II and paradigm II-2, only the timing of the stimulus offset was different from each other. In paradigm II-2, disappearing the stimulus was triggered by saccade onset (Fig. 2A). During the experiment, the saccade onset was defined as the time when the monkey broke the fixation and his eyes moved out from the 1.5° × 1.5° window.

We recorded 23 neurons in MST during paradigms I-2 and II-2. All of the neurons increased their activities after saccades, even when the visual stimulus had already gone [*SI Text, Spatial Tuning Curves of the Neuronal Responses*]. In paradigm I-2, the neuronal population responded to the stimulus similarly when the visual stimulus was turned on in the RF1 and when the saccade brought the stimulus into the RF2 (postresponse/preresponse ratio = $85.9 \pm 39.8\%$; median $\pm$ SD; Fig. S4A). When the moving grating was turned off before saccades in paradigm II-2, most MST neurons still discharged when a saccade brought the location of the visual stimulus into their RFs (postresponse/preresponse ratio = $70.8 \pm 32.2\%$; median $\pm$ SD; Fig. S4B). There was no significant difference between the results obtained by the CRT display (Fig. S3 A and B) and the mirror galvanometers (Fig. S4 A and B) (two-sided Wilcoxon rank sum, $P > 0.05$).

To compare with the results from the CRT display and the mirror galvanometer system, we applied the sliding-window receiver operating characteristic (ROC) analysis to the data obtained from individual trials throughout the period of saccades during paradigm II-2 (*Materials and Methods*). Fig. S4C illustrates the time course of the area under the ROC curve (AUC) as a classifier for the stimulus in RF1 and RF2. For MST neurons ($n = 23$), the AUC for RF1 increased after the stimulus onset and remained high before the saccade and then waned after the saccade, and the AUC for RF2 significantly increased after the saccade offset. The median AUC from 50 to 100 ms after the saccade offset was 0.88 ± 0.29 (Fig. S4D). Thus, no significant difference was observed between the results obtained by the CRT display (Fig. 5B) and the mirror galvanometers (Fig. S4D) (two-sided Wilcoxon rank sum, $P > 0.05$). Therefore, the results support the assumption that the responses after the saccade were evoked by the memory of the preexisted stimuli, but not by the persisted phosphor of the CRT display.

1. Funahashi S, Bruce CJ, Goldman-Rakic PS (1990) Visuospatial coding in primate prefrontal neurons revealed by oculomotor paradigms. *J Neurophysiol* 63(4): 814–831.

2. Inaba N, Shinomoto S, Yamane S, Takemura A, Kawano K (2007) MST neurons code for visual motion in space independent of pursuit eye movements. *J Neurophysiol* 97(5): 3473–3483.
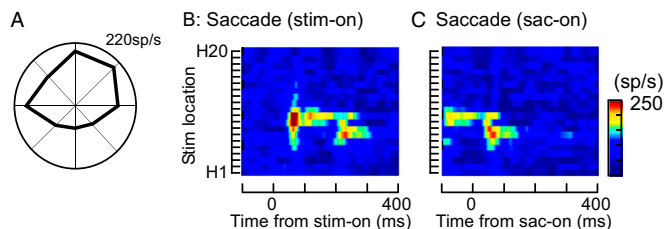
Fig. S1. (*A*) Polar plot of the direction tuning of the MST neuron shown in Figs. 1–3 defined by a moving random-dot pattern in eight directions during fixation. (*B* and *C*) Spatiotemporal RF map of the MST neuron during leftward 10° saccade. Responses are aligned at stimulus onset (*B*) or saccade onset (*C*).
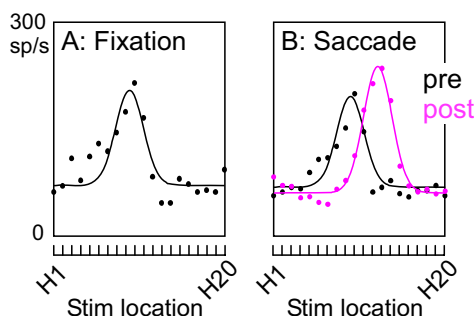

Fig. S2. (*A*) Spatial tuning curves of the neuronal responses of the MST neuron to the moving stimulus located at 20 horizontal locations in the fixation task. Each point shows the mean firing rate over a period from 50 to 150 ms after the stimulus onset. (*B*) Spatial tuning curves of the MST neuron in the saccade task of paradigm I. Each point shows the mean firing rate over a period from 50 to 150 ms after the stimulus onset (black) and 50–150 ms after the saccade onset (magenta), respectively.
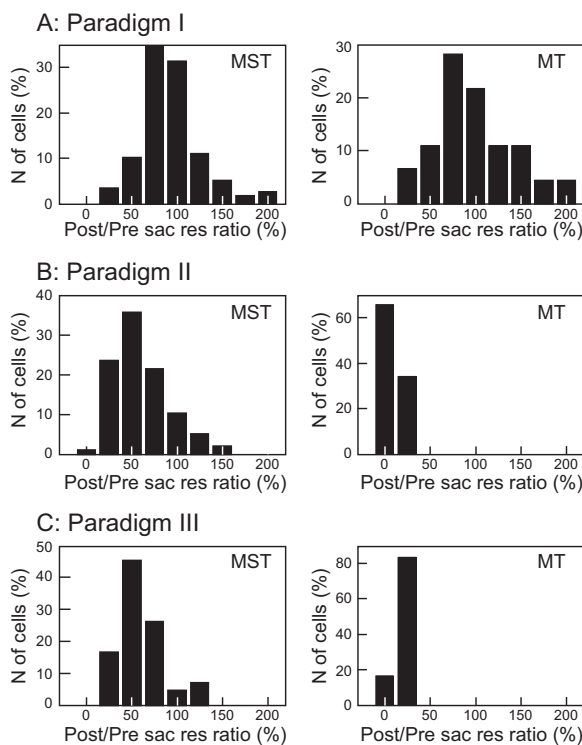

Fig. S3. Comparison of postresponse/preresponse ratio between MST and MT neurons. (*A*–*C*) Distribution of the postresponse/preresponse ratio of MST (*Left*) and MT (*Right*) neurons. (*A*) Paradigm I, (*B*) paradigm II, and (*C*) paradigm III.
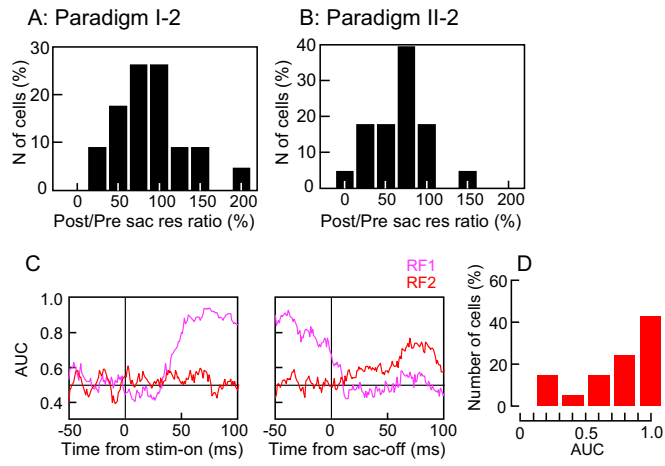
Fig. S4. (*A* and *B*) Distribution of the postresponse/preresponse ratio of the 23 MST neurons. (*A*) Paradigm I-2 and (*B*) paradigm II-2. (*C*) The time course of the AUC as a classifier for the stimulus in RF1 (magenta) and RF2 (red). For MST neurons, the AUC for RF2 significantly increased after the saccade. (*D*) Distribution of the mean AUC from 50 to 100 ms after the saccade offset for the MST neurons.